Published in final edited form as:
Eur J Neurosci. 2014 October ; 40(8): 3202–3214. doi:10.1111/ejn.12690.

Cannabinoid modulation of alpha$_2$ adrenergic receptor function in rodent medial prefrontal cortex

Alessandra M. Cathel[1], **Beverly A. S. Reyes**[2], **Qin Wang**[3], **Jonathan Palma**[1], **Kenneth Mackie**[4], **Elisabeth J. Van Bockstaele**[2], and **Lynn G. Kirby**[1]

[1]Department of Anatomy and Cell Biology, Center for Substance Abuse Research, Temple University School of Medicine, 3500 N. Broad Street, Philadelphia, PA 19140, USA

[2]Department of Pharmacology and Physiology, Drexel University College of Medicine, Philadelphia, PA, USA

[3]Department of Cell, Developmental and Integrative Biology, University of Alabama at Birmingham, Birmingham, AL, USA

[4]Department of Psychological and Brain Sciences, Indiana University, Bloomington, IN, USA

Abstract

Endocannabinoids acting at the cannabinoid type 1 receptor (CB1R) are known to regulate attention, cognition and mood. Previous studies have shown that, in the rat medial prefrontal cortex (mPFC), CB1R agonists increase norepinephrine release, an effect that may be attributed, in part, to CB1Rs localized to noradrenergic axon terminals. The present study was aimed at further characterizing functional interactions between CB1R and adrenergic receptor (AR) systems in the mPFC using *in-vitro* intracellular electrophysiology and high-resolution neuroanatomical techniques. Whole-cell patch-clamp recordings of layer V/VI cortical pyramidal neurons in rats revealed that both acute and chronic treatment with the synthetic CB1R agonist WIN 55,212-2 blocked elevations in cortical pyramidal cell excitability and increases in input resistance evoked by the α2-adrenergic receptor (α2-AR) agonist clonidine, suggesting a desensitization of α2-ARs. These CB1R–α2-AR interactions were further shown to be both action potential- and gamma-aminobutyric acid-independent. To better define sites of cannabinoid–AR interactions, we localized α2A-ARs in a genetically modified mouse that expressed a hemoagglutinin (HA) tag downstream of the α2A-AR promoter. Light and electron microscopy indicated that HA-α2A-AR was distributed in axon terminals and somatodendritic processes especially in layer V of the mPFC. Triple-labeling immunocytochemistry revealed that α2A-AR and CB1R were localized to processes that contained dopamine-β-hydroxylase, a marker of norepinephrine. Furthermore, HA-α2A-AR was localized to processes that were directly apposed to CB1R. These findings suggest multiple sites of interaction between cortical cannabinoid–adrenergic systems that may contribute to understanding the effect of cannabinoids on executive functions and mood.

Correspondence: Lynn G. Kirby, as above., lkirby@temple.edu.

The authors have no conflicts of interests to declare.

Keywords

electron microscopy; electrophysiology; immunohistochemistry; mouse; rat

Introduction

Cannabinoids acting at the cannabinoid type 1 receptor (CB1R) are reported to impact a variety of behavioral states associated with prefrontal cortex function including attention, cognition and anxiety (Witkin *et al.*, 2005; Pattij *et al.*, 2008). The use of cannabis in humans has been associated with impairments in attention and executive function including working memory and cognitive flexibility (see Egerton *et al.*, 2006; Crean *et al.*, 2011) as well as changes in anxiety state (see Hill & Gorzalka, 2009). Preclinical data have also shown similar impairments in attention and cognitive tasks as well as altered behavior in anxiety models in response to stimulation of the CB1R in several animal species (Egerton *et al.*, 2006; Hill & Gorzalka, 2009). Noradrenergic projections from the locus coeruleus to the medial prefrontal cortex (mPFC) have also been linked to these behaviors (Robbins, 1984; Aston-Jones, 1985), and the pathophysiology and treatment of anxiety disorders and disorders of cognition and attention including schizophrenia and attention-deficit hyperactivity disorder are associated with prefrontal cortex norepinephrine (NE) neurotransmission (Zhang *et al.*, 2000; Westerink *et al.*, 2001; Bymaster *et al.*, 2002; Ramos & Arnsten, 2007; Dell·osso *et al.*, 2010; Arnsten & Pliszka, 2011; Gamo & Arnsten, 2011; Arnsten, 2011). To better understand these cannabinoid effects, work in our laboratory has begun to elucidate the interactions between CB1Rs and the NE system in the mPFC. Previous studies showed that WIN 55,212-2, a CB1R agonist, increases cortical NE efflux, an effect that may be mediated by CB1R-mediated desensitization of α2-adrenergic receptors (α2-ARs) (Oropeza *et al.*, 2005; Page *et al.*, 2007; Page *et al.*, 2008). Furthermore, acute exposure to WIN 55,212-2 blocks α2-AR-mediated responses in cortical pyramidal neurons (Reyes *et al.*, 2012). Finally, repeated systemic administration of WIN 55,212-2 has been shown to alter adrenergic receptor expression in the mPFC, increasing β1 adrenergic receptors immediately following treatment but decreasing them 1 week later (Reyes *et al.*, 2009).

Earlier work from others showed that stimulation of α2-ARs enhances the excitability of mPFC pyramidal neurons coupled with an increase in cellular input resistance (Andrews & Lavin, 2006; Carr *et al.*, 2007). These effects were attributed to postsynaptic α2-ARs that inhibited a hyperpolarization/cyclic nucleotide-gated channel-mediated inward current in mPFC pyramidal neurons (Carr *et al.*, 2007). The authors further proposed that mPFC neurons are disinhibited by α2-ARs located on inhibitory gamma-aminobutyric acid (GABA) interneurons (Andrews & Lavin, 2006).

The current study used electrophysiological recordings of pyramidal neurons in a rat mPFC brain slice preparation to examine the effect of acute and chronic CB1R stimulation on α2-AR function as well as the role of GABA in these effects. Next, we characterized the expression of α2-ARs and CB1Rs in rodent mPFC using dual immunohistochemical methods. Hemoagglutinin (HA)-tagged α2A-AR knock-in mice (Lu *et al.*, 2009) were used

for anatomical studies because of the superior specificity of this gene-targeting approach over currently available adrenergic receptor antibodies (Hamdani & van, V, 2009; Jensen *et al.*, 2009; Pradidarcheep *et al.*, 2009). This work provides new information about the regulation of cortical noradrenergic transmission by cannabinoids and may contribute to a better understanding of the mechanisms and circuitry whereby cannabinoids modulate attention, cognition and anxiety.

Materials and methods

Animals

For electrophysiology experiments, male Sprague-Dawley rats (Taconic Farms, Germantown, NY, USA) arrived at 3–4 weeks of age and were housed three per cage under standard temperature and humidity conditions on a 12 h light/dark cycle (lights on at 07:00 h). Food and water were provided *ad libitum*. Animal protocols were approved by the Temple University Institutional Animal Care and Use Committee and were conducted in accordance with the National Research Council *Guide for the Care and Use of Laboratory Animals*.

Seven male HA epitope-tagged wild-type α2A-AR knock-in mice were kindly provided by Dr Qin Wang (University of Alabama, Birmingham, AL, USA). Upon arrival at Thomas Jefferson University Animal Facility, these mice were housed three to a cage (20 °C, 12 h light/dark cycle, lights on at 07:00 h) and were quarantined prior to perfusion at 6 months of age. These mice were used for examining the localization of HA epitope-tagged α2A-AR and cellular associations with CB1R and dopamine-β-hydroxylase (DβH). Food and water were freely available. All procedures conformed to The Institutional Animal Care and Use Committee at Thomas Jefferson University according to the revised *Guide for the Care and Use of Laboratory Animals* (1996), The Health Research Extension Act (1985) and the PHS Policy on Humane Care and Use of Laboratory Animals (1986). All efforts were made to utilize only the minimum number of animals necessary to produce reliable scientific data.

Drugs

For chronic CB1R/vehicle treatment, rats were treated with the synthetic CB1R agonist WIN 55,212-2 (3 mg/kg, i.p.) or vehicle (5% dimethylsulfoxide in 0.9% saline) once daily for 7 days. At 1 h following the seventh injection, rats were killed and brains prepared for electrophysiology. For *in-vitro* electrophysiology, stock solutions of drugs were prepared in dH_20 at 1000× the final concentration and stored in aliquots at −80 °C (WIN 55,212-2, clonidine and bicuculline) or 4 °C [tetrodotoxin (TTX)] until the day of the experiment. A stock solution of SR 141716A (1 mM) was prepared in dimethylsulfoxide (5%) and diluted on the day of the experiment to a final concentration of 1 μM in 0.005% dimethylsulfoxide. Except for chronic CB1R/vehicle treatment, all other drugs were bath applied with the following final concentrations (in μM): 1 WIN 55,212-2, 10 clonidine, 20 bicuculline and 1 TTX. Most drugs and chemicals for the artificial cerebrospinal fluid (ACSF) and electrolyte solutions were obtained from Sigma-Aldrich (St Louis, MO, USA) with the exception of TTX (EMD Chemicals, Inc., Gibbstown, NJ, USA).

Electrophysiology

Subjects (4–5 weeks old) were rapidly decapitated and the head was placed in ice-cold ACSF in which sucrose (248 mM) was substituted for NaCl. The brain was rapidly removed and trimmed to isolate the mPFC. Coronal slices (250 μm thick) containing the infralimbic and prelimbic divisions of the prefrontal cortex were cut on a Vibratome 3000 Plus (Vibratome, St Louis, MO, USA) and placed in ACSF at 35 °C bubbled with 95% O_2/5% CO_2 for 1 h. Slices were then maintained in ACSF at room temperature bubbled with 95% O_2/5% CO_2. The composition of the ACSF was as follows (in mM): 124 NaCl, 2.5 KCl, 2 NaH_2PO_4, 2.5 $CaCl_2$, 2 $MgSO_4$, 10 dextrose and 26 $NaHCO_3$.

Slices were transferred to a recording chamber (Warner Instruments, Hamden, CT, USA) and continuously perfused with ACSF at 1.5–2.0 mL/min at 32–34 °C maintained by an in-line solution heater (TC-324; Warner Instruments, Hamden, CT, USA). Data were obtained from one to three brain slices per rat but only one cell was recorded per brain slice. Pyramidal cells in layer V/VI of the mPFC were visualized using a Nikon E600 upright microscope fitted with a 40× water-immersion objective, differential interference contrast and infrared filter (Optical Apparatus, Ardmore, PA, USA) connected to a CCD camera and computer monitor. Pyramidal cells were identified by their pyramidal-shaped soma and long apical dendrite projecting toward the brain surface as well as their location within mPFC layers V/VI. Whole-cell recording pipettes were made on a P-97 micropipette puller (Sutter Instruments, Novato, CA, USA) using borosilicate glass capillary tubing (1.2 mm outer diameter, 0.69 mm inner diameter; Warner Instruments). The resistance of the electrodes was 4–8 MΩ when filled with an intracellular solution containing (in mM): 120 K-gluconate, 10 KCl, 1 $MgCl_2$, 10 EGTA, 10 HEPES, 2 MgATP, 0.5 Na_2GTP, 10 Na phosphocreatinine and 0.1% biocytin, pH 7.3. A visualized cell was approached with the electrode, a GΩ seal established, and the cell membrane ruptured to obtain a whole-cell recording using a HEKA patch-clamp EPC-10 amplifier (HEKA Elecktronik, Pfalz, Germany) under current-clamp (I = 0 pA) conditions. The series resistance was monitored throughout the experiment. The cell was discarded if the series resistance was unstable or exceeded four times the electrode resistance. Signals were stored on-line using Pulse software, filtered at 1 kHz and digitized at 10 kHz. The liquid junction potential was approximately 9 mV between the pipette solution and the ACSF and was not subtracted from the data obtained.

At baseline, the membrane potential was recorded and input resistance calculated using the current–voltage relationship. Neuronal excitability was assessed in each cell by injecting a series of current pulses (25–625 pA) to determine the current step that would evoke two to three action potentials in the cell. This current step was then used to test neuronal excitability throughout the rest of the experiment. The membrane potential, input resistance and neuronal excitability were also measured following bath application of the α2-AR agonist clonidine (10 μM). To test the effects of acute CB1R stimulation *in vitro*, WIN 55,212-2 (1 μM) was added to the perfusion bath at 6 min prior to clonidine. Clonidine and WIN 55,212-2/clonidine experiments were run at the same time and under identical experimental conditions. In a separate experiment, the role of GABA in α2–cannabinoid type 1 (CB1) interactions or the action-potential-dependent nature of those interactions was

evaluated by measuring the effect of clonidine (10 μM) with WIN 55,212-2 (1 μM) pretreatment in the presence of the $GABA_A$ antagonist bicuculline (20 μM) or TTX (1 μM), respectively. Following some electrophysiological experiments, the pyramidal cell morphology and location of recorded cells were confirmed using standard fluorescence immunohistochemistry techniques (Kirby *et al.*, 2008). The biocytin-filled neuron was visualized with an Alexa Fluor 488-conjugated streptavidin secondary antibody and images captured with a Nikon E800 fluorescent microscope (Nikon Instruments, Melville, NY, USA), using a Retiga EXi Fast 1394 digital camera and QCapture Suite imaging software (Quantitative Imaging Corp., Surrey, BC, Canada).

Electrophysiology data analysis

Electrophysiological recordings were analyzed using Clampfit 9.2 (Axon Instruments, Foster City, CA, USA). Drug effects on membrane voltage, input resistance or neuronal excitability were tested by paired two-tailed Student's t-test. For the chronic pretreatment study, data were analyzed by two-way repeated-measures ANOVA with chronic pretreatment as a between-subjects factor and *in-vitro* drug treatment as a within-subjects factor. Posthoc Student–Newman–Keuls tests were used to compare treatment groups when appropriate. When data did not have a normal distribution or equal variance, equivalent non-parametric tests were employed (i.e. Wilcoxon signed-rank test). All statistical analyses were performed with SigmaPlot 12.5 (Systat Software Inc., San Jose, CA, USA).

Light and immunoelectron microscopy

Four HA-α2A-AR knock-in mice were deeply anesthetized with sodium pentobarbital (40 mg/kg) and perfused transcardially through the ascending aorta with 10 mL heparinized saline followed by 25 mL of 3.75% acrolein (Electron Microscopy Sciences, Fort Washington, PA, USA) and 25 mL of 2% formaldehyde in 0.1 M phosphate buffer (PB) (pH 7.4). The brains were removed immediately after perfusion fixation, sectioned into 1–3 mm coronal slices, postfixed for 30 min and, if necessary, stored in 0.1 M PB (pH 7.4) for a short period prior to sectioning. Sections were cut in the coronal plane at a setting of 40 μm using a Vibratome (Technical Product International, St Louis, MO, USA) and collected into 0.1 M PB.

Sections (40 μm thick through the rostrocaudal extent of the mPFC) were processed for either light microscopic detection of HA or electron microscopic analysis of HA. Sections containing the mPFC that were processed for immunoelectron microscopy were not incubated in any permeabilization agents (e.g. Triton X-100). Tissue sections were incubated in mouse anti-HA (Covance, Emeryville, CA, USA) at 1 : 1000 in 0.1% bovine serum albumin (BSA) and 0.1 M Tris-buffered saline (TBS) (pH 7.6) for 15–18 h at room temperature. The following day, tissue sections were rinsed three times in 0.1 M TBS and incubated in biotinylated donkey anti-mouse (1 : 400; Vector Laboratories, Burlingame, CA, USA) for 30 min followed by rinses in 0.1 M TBS. Subsequently, a 30 min incubation of avidin–biotin complex (Vector Laboratories) was performed. For all incubations and washes, sections were continuously agitated with a rotary shaker. HA-α2A-AR was visualized by a 4 min reaction in 22 mg of 3,3′-diaminobenzidine (Sigma-Aldrich) and 10 μL of 30% hydrogen peroxide in 100 mL of 0.1 M TBS. Some sections were collected,

dehydrated and coverslipped with Permount (Sigma-Aldrich) for light microscopic analysis of HA-α2A-AR immunoreactivity.

Sections were rinsed three times with 0.1 M TBS, followed by rinses with 0.1 M PB and 0.01 M phosphate-buffered saline (PBS) (pH 7.4). Following rinses, sections were then incubated in a 0.2% gelatin–PBS and 0.8% BSA buffer for 10 min and rinsed again in 0.01 M PBS followed by 0.1 M PB. Sections were incubated in 2% osmium tetroxide (Electron Microscopy Sciences) in 0.1 M PB for 1 h, washed in 0.1 M PB, dehydrated in an ascending series of ethanol followed by propylene oxide and flat embedded in Epon 812 (Electron Microscopy Sciences) (Leranth & Pickel, 1989).

Some sections that were not processed for immunoperoxidase labeling were processed for gold–silver localization of HA-α2A-AR. Sections were rinsed three times with 0.1 M TBS, followed by rinses with 0.1 M PB and 0.01 M PBS and were incubated in a 0.2% gelatin–PBS and 0.8% BSA buffer for 10 min. This was followed by incubation in goat anti-mouse IgG conjugate in <1 nm gold particles (Amersham Bioscience Corp., Piscataway, NJ, USA) at room temperature for 2 h. Sections were then rinsed in buffer containing the same concentration of gelatin and BSA as above and subsequently rinsed with 0.01 M PBS. Sections were then incubated in 2% glutaraldehyde (Electron Microscopy Sciences) in 0.01 M PBS for 10 min followed by washes in 0.01 M PBS and 0.2 M sodium citrate buffer (pH 7.4). A silver enhancement kit (Amersham Bioscience Corp.) was used for silver intensification of the gold particles. The optimal times for silver enhancement were determined by empirical observation for each experiment and ranged from 7 to 8 min. Following intensification, tissue sections were rinsed in 0.2 M citrate buffer and 0.1 M PB, and incubated in 2% osmium tetroxide (Electron Microscopy Sciences) in 0.1 M PB for 1 h, washed in 0.1 M PB, dehydrated in an ascending series of ethanol followed by propylene oxide and flat embedded in Epon 812. Thin sections (approximately 50–100 nm thick) were cut with a diamond knife (Diatome-US, Fort Washington, PA, USA) using a Leica Ultracut (Leica Microsystems, Wetzlar, Germany). Sections were collected on copper mesh grids and counterstained with 5% uranyl acetate followed by Reynold's lead citrate. Captured images of selected sections were compared with captured light microscopic images of the block face before sectioning. Sections were examined with a Morgagni (Fei Company, Hillsboro, OR, USA) and digital images were captured using the Advantage HR/HR-B CCD camera system (Advance Microscopy Techniques Corp., Danvers, MA, USA). Figures were assembled and adjusted for brightness and contrast in Adobe Photoshop.

Immunofluorescence microscopy

Three HA epitope-tagged α2A-AR (HA-α2A-AR) knock-in mice were deeply anesthetized with sodium pentobarbital (40 mg/kg; Ovation Pharmaceuticals, Inc., Deerfield, IL, USA) and transcardially perfused through the ascending aorta with 10 mL heparinized saline followed by 25 mL of 4% formaldehyde in 0.1 M PB (pH 7.4). Brains were removed, blocked, postfixed in 4% formaldehyde overnight at 4 °C and stored in 30% sucrose solution in 0.1 M PB containing sodium azide at 4 °C for a few days. The brain was frozen using Tissue Freezing Medium (Triangle Biomedical Science, Durham, NC, USA). Frozen 40-μm-thick sections were cut in the coronal plane using a freezing microtome (Micron HM550

cryostat, Richard-Allan Scientific, Kalamazoo, MI, USA) and collected in 0.1 M PB. Immunofluorescence was performed to visualize CB1, HA-α2A-AR and DβH in the mPFC. Briefly, tissue sections were placed for 30 min in 1% sodium borohydride in 0.1 M PB to reduce amine-aldehyde compounds. The tissue sections were then incubated in 4.0% normal donkey serum and 0.25% Triton X-100 in 0.1 M TBS (pH 7.6) for 30 min. Thorough rinses in 0.1 M TBS were performed following incubation. Subsequently, sections were incubated in guinea pig anti-CB1R (Dr Ken Mackie, Indiana University, Bloomington, IN, USA) at 1 : 1000, mouse anti-HA-α2A-AR (Covance) at 1 : 1000 and rabbit anti-DβH (Abcam, Cambridge, MA, USA) at 1 : 1000 in 0.1% BSA and 0.25% Triton X-100 in 0.1 M TBS. The incubation time was 15–18 h in a rotary shaker at room temperature. Sections were then washed in 0.1 M TBS and incubated in a secondary antibody cocktail containing fluorescein isothiocyanate donkey anti-mouse (1 : 200; Jackson ImmunoResearch Laboratories Inc., West Grove, PA, USA), tetramethyl rhodamine isothiocyanate donkey anti-guinea pig (1 : 200; Jackson ImmunoResearch Laboratories Inc.) and Cy5 donkey anti-rabbit antibodies prepared in 0.1% BSA and 0.25% Triton X-100 in 0.1 M TBS for 2 h in the dark on a rotary shaker. Following incubation with the secondary antibodies, the tissue sections were rinsed in 0.1 M TBS, mounted on slides and allowed to dry. The slides were dehydrated in a series of alcohols soaked in xylene, coverslipped using DPX (Sigma-Aldrich Inc., St Louis, MO, USA) and tissue sections were examined using a confocal microscope (LSM 510 Meta, Carl Zeiss Inc., Thornwood, NY, USA) to visualize the immunofluorescence labeling. Figures were assembled and adjusted for brightness and contrast in Adobe Photoshop.

Controls and immunohistochemical data analysis

Some sections were used for control experiments and were processed without exposure to the primary antibody. These sections were processed in parallel with tissue sections incubated in the primary antibody. To evaluate cross-reactivity of the primary antisera by secondary antisera, some sections were processed for dual labeling with omission of one of the primary antisera. Tissue sections from mice with good preservation of ultrastructural morphology and with marker clearly apparent were used for the analysis. The quantification of HA-α2A-AR-immunolabeled profiles was carried out at the plastic–tissue interface to ensure that immunolabeling was detectable in all sections used for analysis (Chan et al., 1990).

The cellular elements were identified based on the description of Peters and colleagues (Peters *et al.*, 1991; Peters & Palay, 1996). Somata contained a nucleus, Golgi apparatus and smooth endoplasmic reticulum. Proximal dendrites contained endoplasmic reticulum, were postsynaptic to axon terminals and were larger than 0.7 μm in diameter. A terminal was considered to form a synapse if it showed synaptic vesicles near a restricted zone of parallel membranes with slight enlargement of the intercellular space, and/or associated with postsynaptic thickening. Asymmetric synapses were identified by thick postsynaptic densities (Gray's type I) (Gray, 1959); in contrast, symmetric synapses had thin densities (Gray's type II) (Gray, 1959) both presynaptically and postsynaptically. A non-synaptic apposition was defined as an axon terminal plasma membrane juxtaposed to that of a dendrite or soma devoid of recognizable membrane specializations and with no intervening glial processes.

Identification of immunogold–silver labeling in profiles

Selective immunogold–silver-labeled profiles were identified by the presence, in single thin sections, of at least two to three immunogold–silver particles within a cellular compartment. Even if a profile contained immunogold particles in adjacent thin sections, it was designated as lacking detectable immunoreactivity if there were fewer than two to three particles in each section.

Results

α2-adrenergic receptor stimulation of medial prefrontal cortex pyramidal neuron excitability and input resistance

Stimulation of α2-ARs with the selective agonist clonidine (10 μM) increased mPFC pyramidal neuron excitability and input resistance *in vitro* (Fig. 1). There was no significant effect of clonidine on the mean membrane voltage (baseline, −71.7 ± 2.6 mV; clonidine, −71.8 ± 2.5 mV). Clonidine increased the number of evoked action potentials in response to a current step in an individual mPFC pyramidal neuron from 2 to 5 spikes/pulse (Fig. 1A) and significantly elevated the mean neuronal excitability ($t_5 = -3.25$, $p = 0.02$; Fig. 1B; N = 6 cells recorded from four rats). Clonidine also increased the input resistance in an individual mPFC pyramidal neuron from 157 to 251 MΩ, as shown by voltage responses to a series of hyperpolarizing to depolarizing current steps (Fig. 1C; −100 to 160 pA) and summarized in the current–voltage plot (Fig. 1C′) and significantly elevated mean input resistance ($t_4 = -5.16$, $p = 0.007$; Fig. 1D; N = 6 cells recorded from four rats).

Acute cannabinoid type 1 receptor blockade of α2-adrenergic receptor effects on medial prefrontal cortex pyramidal neurons

Acute stimulation of CB1R *in vitro* with the agonist WIN 55,212-2 (1 μM) depolarized mPFC pyramidal neurons (baseline, −70.3 ± 2.2 mV; WIN 55,212-2, −67.6 ± 2.7 mV; $t_8 = -2.39$, $p = 0.04$; N = 9 cells recorded from six rats; data not shown) but the clonidine treatment that followed produced no further effect on membrane voltage (clonidine, −69.1 ± 2.0 mV). This WIN 55,212-2-induced depolarization was not accompanied by a change in mPFC pyramidal neuron excitability or input resistance. However, in the presence of WIN 55,212-2, the effects of clonidine on mPFC pyramidal neuron excitability and input resistance (Fig. 1) were blocked (Fig. 2). Following WIN 55,212-2 pretreatment, clonidine did not significantly elevate the mean mPFC pyramidal neuron excitability (N = 7 cells recorded from five rats; Fig. 2A) or input resistance (N = 9 cells recorded from six rats; Fig. 2B) above either the WIN 55,212-2 or predrug baseline. To confirm the receptor mediating the blockade of clonidine effects by WIN 55,212-2, this experiment was repeated in slices preincubated for 2 h in the selective CB1R antagonist SR 141716A (1 μM) or vehicle. In the presence of vehicle (N = 6), WIN 55,212-2 blocked the clonidine response as described above; in slices pretreated with vehicle + WIN 55,212-2, clonidine had no effect on the mPFC pyramidal neuron excitability, input resistance or membrane voltage. By contrast, in the presence of SR 141716A (N = 8), WIN 55,212-2 had no effect on the clonidine response. Specifically, in the presence of both SR 141716A and WIN 55,212-2, clonidine elevated the mPFC pyramidal neuron excitability from 1.58 ± 0.71 to 3.71 ± 0.88 spikes/pulse ($t_7 = -3.75$, $p = 0.007$) and increased the input resistance from 153.8 ± 32.9 to 176.2 ± 33.3 MΩ

($t_7 = -2.84$, $p = 0.02$), although there was no effect of clonidine on membrane voltage. These data confirm that the WIN 55,212-2 blockade of clonidine is mediated by the CB1R.

Chronic cannabinoid type 1 receptor blockade of α2-adrenergic receptor effects on medial prefrontal cortex pyramidal neurons

Figure 3 indicates that mPFC pyramidal neurons from chronic vehicle controls showed clonidine-induced elevations in the mean mPFC pyramidal neuron excitability and input resistance (N = 17 cells recorded from 12 rats; $p < 0.01$; Fig. 3A and B, respectively), similar to the effects of clonidine on mPFC pyramidal neurons from naive subjects (Fig. 1). In contrast, the effects of clonidine on mPFC pyramidal neuron excitability (N = 10 cells recorded from nine rats; Fig. 3A) and input resistance (N = 9 cells recorded from eight rats; Fig. 3B) were absent in chronic WIN 55,212-2-pretreated subjects. Two-way repeated-measures ANOVA of membrane excitability data indicated significant main effects of chronic drug pretreatment ($F_{1,25} = 7.06$, $p = 0.01$), *in-vitro* drug treatment ($F_{1,25} = 6.73$, $p = 0.02$) and a significant interaction between the two factors ($F_{1,25} = 7.20$, $p = 0.01$). Posthoc Student–Newman–Keuls test indicated a significant elevation of excitability by clonidine in the chronic vehicle group ($p < 0.001$) and a significantly diminished clonidine response in the chronic WIN 55,212-2 group compared with chronic vehicle controls ($p < 0.001$). Two-way repeated-measures ANOVA of input resistance data indicated a significant main effect of *in-vitro* drug treatment ($F_{1,24} = 7.82$, $p = 0.01$) but no effect of chronic drug pretreatment or interaction between the two factors. Posthoc Student–Newman–Keuls test indicated a significant elevation of input resistance by clonidine in the chronic vehicle group ($p = 0.002$). Two-way repeated-measures ANOVA of membrane voltage data (not shown) indicated a significant main effect of *in-vitro* drug treatment ($F_{1,25} = 5.58$, $p = 0.03$) but no effect of chronic drug pretreatment or interaction between the two factors. An acute *in-vivo* WIN 55,212-2 experiment was conducted (1 mg/kg at 1 h prior to brain slice preparation) for comparison with the effects of chronic *in-vivo* WIN 55,212-2. In this group, *in-vitro* clonidine retained its ability to increase both cell excitability (baseline excitability, 3.1 ± 0.2 spikes/pulse vs. clonidine excitability, 5.1 ± 0.8 spikes/pulse; N = 12, $p = 0.02$ by paired Student's t-test) and input resistance (baseline input resistance, 224.7 ± 29.9 MΩ vs. clonidine input resistance, 265.9 ± 43.4 spikes/pulse; N = 9, $p = 0.03$ by paired Student's t-test) in mPFC pyramidal neurons, indicating that the blockade of the α2-adrenergic response by chronic WIN 55,212-2 was not due to the final injection of WIN 55,212-2, which could have remained in the tissue due to its high lipophilicity.

Cannabinoid type 1 receptor–α2-adrenergic receptor interactions are action potential- and GABA-independent

In order to determine whether the WIN 55,212-2 blockade of the effects of clonidine on mPFC pyramidal neurons is direct or mediated through synaptic afferents, we tested the WIN 55,212-2/clonidine drug combinations in the presence of either TTX (1 μM) or bicuculline (20 μM) to block action potentials or $GABA_A$ receptors, respectively. In the presence of TTX, the WIN 55,212-2 blockade of the effects of clonidine on mPFC pyramidal neuron input resistance (N = 8 cells recorded from three rats; Fig. 4A) was similar to that observed in naive or chronic vehicle controls (Figs 1D and 3B). In the presence of bicuculline, the WIN 55,212-2 blockade of the effects of clonidine on mPFC pyramidal

neuron excitability (N = 7 cells recorded from four rats; Fig. 4B) and input resistance (N = 7 cells recorded from four rats; Fig. 4C) was similar to that observed in naive subjects (Fig. 1B and D) and chronic vehicle controls (Fig. 3A and B).

Hemoagglutinin–α2A-AR localization in the medial prefrontal cortex using light and electron microscopy

We used high-resolution neuroanatomical approaches in a genetically modified mouse that places an HA-epitope tag downstream of the α2A-AR promoter to localize the adrenergic receptor in the mPFC (Lu *et al.*, 2009). HA-α2A-AR immunoreactivity was visualized using both immunoperoxidase detection and immunogold–silver labeling in separate sections of tissue in the mPFC (Figs 5–8). In order to ensure the specificity of each of the secondary antibodies employed, control tissue sections were processed in parallel, with omission of the primary antibodies for HA-α2A-AR. In sections lacking the primary antibody, no immunoperoxidase or immunogold–silver labeling was observed following exposure to the secondary antibody alone (data not shown). Using light microscopic visualization of peroxidase-labeled HA-α2A-AR, immunoreactivity was abundant throughout the rostrocaudal levels of the mPFC (Fig. 5) and was particularly enriched in the deeper layers of the neocortex as previously reported (Aoki *et al.*, 1994).

The subcellular distribution of HA-α2A-AR in the mPFC was analyzed (Figs 6–8) using both immunoperoxidase and immunogold–silver. The labeling observed by light microscopy (Fig. 5) indicated that the HA-α2A-AR might reflect antigens located within cell bodies or within fine processes closely associated with mPFC somatodendritic processes. Electron microscopy revealed that peroxidase labeling for HA-α2A-AR was robust within axon terminals (Fig. 6) and appeared as discrete clumps near the rough endoplasmic reticulum and along the intracellular surface of the plasma membrane in somata (Fig. 7) and dendrites (Fig. 8). Within dendrites, peroxidase labeling occurred as discrete patches along the plasma membrane. However, not all of these immunoreactive patches received synaptic contacts from axon terminals. Sections that were processed for silver intensification of HA-α2A-AR showed a similar distribution of immunoreactivity for HA-α2A-AR in axon terminals (Fig. 6) and dendrites (Fig. 8). Of the 1243 profiles exhibiting HA-α2A-AR immunoreactivity, 61.22% (761/1243) were identified as axon terminals, whereas 38.78% (482/1243) were identified as dendritic processes. HA-α2A-AR was also observed within the cytoplasmic compartment of somata (Fig. 7) but the frequency of distribution was not included in the analysis.

Triple-immunofluorescence studies were conducted in the same section of tissue in the mPFC to examine the potential co-existence of HA-α2A-AR, CB1R and DβH using three distinct fluorophore-tagged secondary antibodies (Fig. 9). HA-α2A-AR immunoreactivity was distributed throughout the rat mPFC (Fig. 9A and D). We confirmed earlier neuroanatomical studies (Oropeza et al., 2007; Reyes et al., 2009; Richter et al., 2012) showing that noradrenergic terminals contain CB1R. Here, we provide the first evidence of multiple examples of cortical noradrenergic DβH-labeled terminals expressing both α2A-AR and CB1R. In addition, cellular processes lacking DβH immunoreactivity contained α2A-AR or CB1R. These processes could be axon terminals containing a transmitter other than

NE or could be postsynaptic processes. Future studies using triple-labeling immunoelectron microscopy are required to determine the frequency of association of α2A-AR and CB1R in presynaptic vs. postsynaptic neurons in the mPFC.

Discussion

The present study indicates functional desensitization of α2-ARs on layer V/VI pyramidal cells in the mPFC by CB1R agonism and provides anatomical evidence for multiple sites of interaction between CB1Rs and α2A-ARs within the mPFC involving both presynaptic and postsynaptic mechanisms. These presynaptic and postsynaptic interactions can account for both the current electrophysiology findings and our earlier studies indicating CB1R-mediated stimulation of mPFC NE efflux.

We confirmed earlier demonstrations that the α2-AR agonist clonidine, administered *in vitro*, increases the excitability of pyramidal neurons coupled with an increase in input resistance, reflecting inhibition of an HCN-mediated inward current (Carr *et al.*, 2007). Similar α2-AR effects in the mPFC have also been found in other species and with other α2-AR agonists including guanfacine and methylphenidate (Li *et al.*, 1999; Andrews & Lavin, 2006; Wang *et al.*, 2007). We further demonstrated that acute and chronic stimulation of CB1R produces a functional desensitization of α2-ARs on pyramidal neurons in the mPFC by preventing the effect of clonidine on pyramidal cell excitability and input resistance. It is also notable that, despite marked drug time-course differences between the rapid onset of CB1R stimulation *in vitro* vs. the slower onset *in vivo* for acute vs. chronic studies, respectively, the desensitization of α2-ARs was similar. The CB1R desensitization of the effects of clonidine is unchanged by action potential blockade with TTX or by blockade of $GABA_A$ receptors, ruling out CB1 interactions with α2-ARs located on GABAergic interneurons. High-resolution anatomical analysis indicated multiple sites of interactions between the receptor systems.

Methodological considerations

Through molecular cloning, the existence of three distinct subtypes of α2-ARs (α2A-AR, α2B-AR and α2C-AR) have been described (Bylund *et al.*, 1992). Due to limitations in pharmacological tools, it has been difficult to ascribe the role of each subtype to the central functions of α2-AR. *In-situ* hybridization studies have provided valuable information regarding their distribution within the brain. However, little is known about their subcellular distribution and, in particular, their presynaptic vs. postsynaptic localization or their relation to noradrenergic neurons in the central nervous system. Aoki *et al.* (1994) used an antiserum that selectively recognized the A-subtype of α2-AR to determine immunoreactivity in monkey cortex and reported that α2A-AR immunoreactivity occurred as small puncta, less than 1 μm in diameter, that cluster over neuronal perikarya. Subcellularly, they reported that α2A-AR-immunoreactivity in the mPFC was associated with the synaptic and non-synaptic plasma membrane of dendrites and perikarya as well as perikaryal membranous organelles. In addition, cortical tissue exhibited prominent immunoreactivity within spine heads.

Both rats and mice were used in these experiments. Rats were used for electrophysiology studies in order to confirm previous demonstrations of the α2-AR-mediated excitability of

rat cortical pyramidal neurons (Carr *et al.*, 2007) and examine their regulation by CB1 agonists in the brain slice preparation. HA epitope-tagged wild-type α2A-AR knock-in mice were used for anatomical studies because of the current lack of selective antibodies for adrenergic receptors (Hamdani & van der Velden, 2009; Jensen *et al.*, 2009; Pradidarcheep *et al.*, 2009). However, the pattern of expression for mRNA encoding α2A-AR in the adult mouse brain is very similar to that reported for the expression of α2A-AR mRNA in rat brain (McCune *et al.*, 1993; Nicholas *et al.*, 1993; Scheinin *et al.*, 1994). Electrophysiology experiments were also conducted in juvenile subjects due to limitations of brain slice viability at older ages (Alger *et al.*, 1984; Gibb & Edwards, 1994). However, cortical CB1Rs and α2A-ARs are both fully functional (i.e. coupled to signal transduction pathways) in the juvenile rat brain (Berrendero *et al.*, 1998; Winzer-Serhan & Leslie, 1999), and thus the electrophysiology data in juveniles probably reflect mature receptor interactions. The findings from both age groups also underscore the importance of cannabinoid–adrenergic interactions throughout development.

Specificity of antibodies and control sections

The CB1R used in this study was labeled with an affinity-purified polyclonal antibody raised in guinea pig against its C-terminus. The specificity and characterization of the CB1R have been previously established (Katona *et al.*, 2006; Fitzgerald *et al.*, 2012; Fitzgerald *et al.*, 2013). Immunoperoxidase labeling for CB1R was carried out in CB1R−/− mice in multiple brain regions to verify the lack of immunoreactivity in knock-out animals. Tissue sections obtained from wild-type mice showed visible immunoperoxidase labeling in several brain regions including the cerebral cortex, striatum and hippocampus (Katona *et al.*, 2006; Fitzgerald *et al.*, 2012). Immunoperoxidase detection of CB1R antibody was performed in tissue sections obtained from the forebrain of CB1R−/− mice in parallel with the tissue sections obtained from the wild-type mice. CB1R immunoreactivity was absent in tissues from CB1R−/− mice. Preadsorption of the primary antisera with corresponding blocking peptide prevented demonstration of CB1R immunoreactivity as compared with the rat forebrain tissue sections in which standard immunohistochemistry was performed. The DβH polyclonal antibody was labeled with an affinity-purified polyclonal antiserum generated in rabbit against amino acids 8 and 290. Western blotting at a concentration of 1–2 μg/mL detects a band of approximately 72 kDa. Immunoperoxidase and immunofluorescence detections of DβH were conducted in sections of mouse brains, and DβH was also expressed in cell cultures (Polanski *et al.*, 2010; Matthews *et al.*, 2013). The monoclonal antibody against HA-α2A-AR was generated in mouse against the 12-amino-acid peptide CYPYDVPDYASL. The antibody recognizes HA epitopes located in the middle of protein sequences as well as at the N-terminus and C-terminus. Using HA-α2A-AR and fluorescence-conjugated secondary antibody, the distribution of HA-α2A-AR in knock-in mouse brain has been demonstrated (Wang & Limbird, 1997; Lu *et al.*, 2009). Furthermore, control of specificity for CB1R, HA-α2A-AR and DβH was also carried out, including control of the secondary antibody where control sections were also processed without primary antibody/ies but with secondary antibody and control for primary antibody/ies where some sections were processed with primary antibody/ies but without secondary antibody/ies. In those control tissue sections, run in parallel, immunofluorescence, peroxidase immunoreactivity or immunogold-silver particles were not demonstrated in

tissue sections from which primary or secondary antibody/ies was/were omitted. To evaluate the possible cross-immunoreactivity of secondary antibodies with the primary antibodies in the dual- or triple-labeling experiment, some sections were processed for dual or triple immunolabeling with omission of one of the primary antibodies.

Functional implications for cannabinoid type 1 receptor–α2-adrenergic receptor interactions at the presynaptic level

The present study indicates that axon terminals expressing α2A-AR co-localize CB1R in axon terminals in the mPFC (Oropeza *et al.*, 2007), confirming reports by others (Richter *et al.*, 2012), and is in agreement with other studies showing a predominant presynaptic distribution of α2-AR in this region (Cerrito & Preziosi, 1985; Dennis *et al.*, 1987; Meana *et al.*, 1992; Pudovkina *et al.*, 2001; Flugge *et al.*, 2004). The present findings build on our earlier studies using *in-vivo* microdialysis indicating that CB1R agonist treatment with WIN-55,212-2 stimulates NE release in the mPFC (Oropeza *et al.*, 2005; Page *et al.*, 2007; Page *et al.*, 2008).

Although our electrophysiology findings do not favor the hypothesis of disinhibition of mPFC NE efflux via desensitization of α2-AR heteroreceptors located on inhibitory GABA interneurons, desensitization of inhibitory presynaptic α2-autoreceptors would also result in the observed stimulation of NE efflux. Regardless of the drug time-course difference between the rapid onset of CB1R stimulation *in vitro* and *in vivo* for acute vs. chronic studies, desensitization of α2-AR occurred in a similar fashion. Desensitization of α2-AR is likely to take place via the sequestration, downregulation and decreases in Gi that have been described following agonist exposure to α2-AR (Jones *et al.*, 1990; Liggett *et al.*, 1992; Jewell-Motz *et al.*, 1998). It is possible that CB1R competes for Gi, rendering less Gi available for α2-AR. It is also possible that α2-AR is phosphorylated by G-protein-coupled receptor kinases and/or second messenger-dependent kinases such as protein kinases A and C (Milligan *et al.*, 1995), considering that persistent activation of phospholipase C and protein kinase C signaling pathways induces firing (Carr *et al.*, 2007). Furthermore, α2-AR may be sequestered to the intracellular compartment (Milligan *et al.*, 1995) that leads to desensitization. Nevertheless, further investigation is needed to determine the exact mechanism by which α2-AR undergoes desensitization following acute or chronic CB1R agonist exposure. When NE is released from the CB1R- and α2-AR-containing axon terminals, it binds with α2-ARs that are localized postsynaptically that could in turn modulate α2-AR postsynaptic adrenoreceptor function. Future studies are necessary to address this concern.

We demonstrated using electron microscopy that α2A-ARs are localized in axon terminals, somata and dendrites in the mPFC, and using dual immunofluorescence we showed CB1–α2A-AR co-localization at multiple sites within the mPFC. Although previous studies in our laboratory have shown CB1R agonist-stimulated downregulation of α2-AR protein expression in the nucleus accumbens by western blot analysis (Carvalho *et al.*, 2010), similar effects were not observed in the prefrontal cortex (Reyes *et al.*, 2009). Additional studies with cellular resolution are needed to determine whether the observed functional desensitization of mPFC α2-ARs by CB1R agonism is mediated by reductions of α2-AR

expression on the cell surface and/or uncoupling of the receptor from intracellular signaling pathways.

Functional implications for cannabinoid type 1 receptor–α2-adrenergic receptor interactions at the postsynaptic level

Evidence for the postsynaptic effects of clonidine on α2-ARs arises from earlier studies indicating that depletion of NE by reserpine has no effect on the clonidine-mediated stimulation of pyramidal cell excitability and input resistance, ruling out the involvement of presynaptic α2-autoreceptors on adrenergic terminals and their modulation of NE release as a site of action for clonidine (Carr *et al.*, 2007). Although suggestive of a postsynaptic site of action, the effects of reserpine are not limited to NE terminals (Bertler, 1961). For additional evidence, we examined CB1R–α2-AR interactions under conditions of synaptic isolation with TTX. When pyramidal neurons were isolated from synaptic influence by either NE terminals or neighboring interneurons, the CB1R–induced desensitization of α2-ARs persisted, supporting a postsynaptic site of action.

The present study also supports the possibility of CB1R–α2-AR interactions occurring via a postsynaptic mechanism similar to that observed in the hypothalamic magnocellular neurosecretory cells (Kuzmiski *et al.*, 2009). In the study by Kuzmiski *et al.* (2009), activation of α2-AR localized postsynaptically engaged postsynaptic Gαi/o-coupled receptors to promote endocannabinoid production through the activation of phospholipase D. The postsynaptic distribution of CB1R has met with some debate.

It is also possible that, based on our previous description of CB1R in dendrites (Scavone *et al.*, 2010) and the known association of β1-ARs with postsynaptic cells (Strader *et al.*, 1983; Aoki *et al.*, 1987; Hu *et al.*, 2000), β1-AR will co-exist with CB1R and endocannabinoid-synthesizing enzymes in dendritic cortical profiles, suggesting an anatomical substrate for functional interactions between the two systems. Physical interactions have been reported between CB1R and β2-AR and, in human embryonic kidney 293H cells, co-expression of β2-AR tempered the constitutive activity and increased cell surface expression of CB1Rs (Hudson *et al.*, 2010).

We also detected CB1R in axon terminals apposed to separately labeled α2-AR-labeled dendrites. Additional immunoelectron microscopy studies are needed to provide a complete picture of putative cellular interactions.

Conclusions

In summary, these studies present evidence of the functional desensitization of postsynaptic α2-ARs on layer V/VI pyramidal cells in the mPFC by CB1R agonism and offer anatomical support for multiple sites of interaction between CB1Rs and α2-ARs within the mPFC at presynaptic terminals as well as somata and dendrites. These presynaptic and postsynaptic interactions can account for both the current electrophysiology findings and earlier studies in the laboratory indicating CB1R-mediated stimulation of mPFC NE efflux. Considering that cortical NE neurotransmission is known to contribute to multiple cognitive and behavioral states including attention and anxiety (Miller & Cohen, 2001; Lapiz & Morilak, 2006; Page *et al.*, 2007; Ramos & Arnsten, 2007; Arnsten *et al.*, 2007), a better understanding of the

circuitry underlying CB1–α2-AR interactions may elucidate the cellular mechanisms underlying cannabinoid-stimulated changes in attention, cognition and anxiety (Verrico *et al.*, 2003; Ranganathan & D'Souza, 2006; D·Souza *et al.*, 2008), and may identify novel targets for the treatment of cognitive–behavioral and anxiety disorders.

Acknowledgments

This work was supported by NIDA DA 20126 (L.G.K.), DA 20129 (E.J.V.B.) and DA 13429.

Abbreviations

α2-AR	α2-adrenergic receptor
ACSF	artificial cerebrospinal fluid
BSA	bovine serum albumin
CB1	cannabinoid type 1
CB1R	cannabinoid type 1 receptor
DβH	dopamine-β-hydroxylase
GABA	gamma-aminobutyric acid
HA	hemoagglutinin
mPFC	medial prefrontal cortex
NE	norepinephrine
PB	phosphate buffer
PBS	phosphate-buffered saline
TBS	Tris-buffered saline
TTX	tetrodotoxin

References

Alger, BE.; Dhanjal, SS.; Dingledine, R.; Garthwaite, J.; Henderson, G.; King, GL.; Lipton, P.; North, A.; Schwartzkroin, PA.; Sears, TA.; Segal, M.; Whittingham, TS.; Williams, J. Appendix: Brain slice methods. In: Dingledine, R., editor. Brain Slices. New York, N.Y: Plenum Press; 1984. p. 381-438.

Andrews GD, Lavin A. Methylphenidate increases cortical excitability via activation of alpha-2 noradrenergic receptors. Neuropsychopharmacology. 2006; 31:594–601. [PubMed: 15999146]

Aoki C, Go CG, Venkatesan C, Kurose H. Perikaryal and synaptic localization of alpha 2A–adrenergic receptor-like immunoreactivity. Brain Res. 1994; 650:181–204. [PubMed: 7953684]

Aoki C, Joh TH, Pickel VM. Ultrastructural localization of beta-adrenergic receptor-like immunoreactivity in the cortex and neostriatum of rat brain. Brain Res. 1987; 437:264–282. [PubMed: 2829995]

Arnsten AF. Catecholamine influences on dorsolateral prefrontal cortical networks. Biol. Psychiatry. 2011; 69:e89–e99. [PubMed: 21489408]

Arnsten AF, Pliszka SR. Catecholamine influences on prefrontal cortical function: relevance to treatment of attention deficit/hyperactivity disorder and related disorders. Pharmacol. Biochem. Behav. 2011; 99:211–216. [PubMed: 21295057]

Arnsten AF, Scahill L, Findling RL. alpha2-Adrenergic receptor agonists for the treatment of attention-deficit/hyperactivity disorder: emerging concepts from new data. J. Child Adolesc. Psychopharmacol. 2007; 17:393–406. [PubMed: 17822336]

Aston-Jones G. Behavioral functions of locus-coeruleus derived from cellular attributes. Physiological Psychology. 1985; 13:118–126.

Berrendero F, Garcia-Gil L, Hernandez ML, Romero J, Cebeira M, de MR, Ramos JA, Fernandez-Ruiz JJ. Localization of mRNA expression and activation of signal transduction mechanisms for cannabinoid receptor in rat brain during fetal development. Development. 1998; 125:3179–3188. [PubMed: 9671590]

Bertler A. Occurrence and localization of catechol amines in human brain. Acta Physiologica Scandinavica. 1961; 51:97.

Bylund DB, Blaxall HS, Iversen LJ, Caron MG, Lefkowitz RJ, Lomasney JW. Pharmacological characteristics of alpha 2-adrenergic receptors: comparison of pharmacologically defined subtypes with subtypes identified by molecular cloning. Mol. Pharmacol. 1992; 42:1–5. [PubMed: 1353247]

Bymaster FP, Katner JS, Nelson DL, Hemrick-Luecke SK, Threlkeld PG, Heiligenstein JH, Morin SM, Gehlert DR, Perry KW. Atomoxetine increases extracellular levels of norepinephrine and dopamine in prefrontal cortex of rat: a potential mechanism for efficacy in attention deficit/hyperactivity disorder. Neuropsychopharmacology. 2002; 27:699–711. [PubMed: 12431845]

Carr DB, Andrews GD, Glen WB, Lavin A. alpha2-Noradrenergic receptors activation enhances excitability and synaptic integration in rat prefrontal cortex pyramidal neurons via inhibition of HCN currents. J. Physiol. 2007; 584:437–450. [PubMed: 17702809]

Carvalho AF, Mackie K, Van Bockstaele EJ. Cannabinoid modulation of limbic forebrain noradrenergic circuitry. Eur. J. Neurosci. 2010; 31:286–301. [PubMed: 20074224]

Cerrito F, Preziosi P. Rat brain alpha 2-pre- and postsynaptic receptors are different or differently modulated? J. Neurosci. Res. 1985; 14:423–431. [PubMed: 2867226]

Crean RD, Crane NA, Mason BJ. An evidence based review of acute and long-term effects of cannabis use on executive cognitive functions. J. Addict. Med. 2011; 5:1–8. [PubMed: 21321675]

D'Souza DC, Ranganathan M, Braley G, Gueorguieva R, Zimolo Z, Cooper T, Perry E, Krystal J. Blunted psychotomimetic and amnestic effects of delta-9-tetrahydrocannabinol in frequent users of cannabis. Neuropsychopharmacology. 2008; 33:2505–2516. [PubMed: 18185500]

Dell'osso B, Buoli M, Baldwin DS, Altamura AC. Serotonin norepinephrine reuptake inhibitors (SNRIs) in anxiety disorders: a comprehensive review of their clinical efficacy. Hum. Psychopharmacol. 2010; 25:17–29. [PubMed: 20041476]

Dennis T, L'Heureux R, Carter C, Scatton B. Presynaptic alpha-2 adrenoceptors play a major role in the effects of idazoxan on cortical noradrenaline release (as measured by in vivo dialysis) in the rat. J. Pharmacol. Exp. Ther. 1987; 241:642–649. [PubMed: 3033221]

Egerton A, Allison C, Brett RR, Pratt JA. Cannabinoids and prefrontal cortical function: insights from preclinical studies. Neurosci. Biobehav. Rev. 2006; 30:680–695. [PubMed: 16574226]

Fitzgerald ML, Mackie K, Pickel VM. The impact of adolescent social isolation on dopamine D2 and cannabinoid CB1 receptors in the adult rat prefrontal cortex. Neuroscience. 2013; 235:40–50. [PubMed: 23333674]

Fitzgerald ML, Shobin E, Pickel VM. Cannabinoid modulation of the dopaminergic circuitry: implications for limbic and striatal output. Prog. Neuropsychopharmacol. Biol. Psychiatry. 2012; 38:21–29. [PubMed: 22265889]

Flugge G, Van KM, Mijnster MJ. Perturbations in brain monoamine systems during stress. Cell Tissue Res. 2004; 315:1–14. [PubMed: 14579145]

Franklin, BJK.; Paxinos, G. The mouse brain in stereotaxic coordinates. San Diego: Academic Press; 2008.

Gamo NJ, Arnsten AF. Molecular modulation of prefrontal cortex: rational development of treatments for psychiatric disorders. Behav. Neurosci. 2011; 125:282–296. [PubMed: 21480691]

Gibb, AJ.; Edwards, FA. Patch clamp recording from cells in sliced tissues. In: Standen, NB., editor. Microelectrode Techniques, the Plymouth Workshop Handbook. Cambridge, UK: Company of Biologists; 1994. p. 255-274.

Gray EG. Axo-somatic and axo-dendritic synapses of the cerebral cortex: an electron microscopic study. J. Anat. 1959; 93:420–433. [PubMed: 13829103]

Hamdani N, van der Velden J. Lack of specificity of antibodies directed against human beta-adrenergic receptors. Naunyn Schmiedebergs Arch. Pharmacol. 2009; 379:403–407. [PubMed: 19156400]

Hill MN, Gorzalka BB. The endocannabinoid system and the treatment of mood and anxiety disorders. CNS Neurol. Disord. Drug Targets. 2009; 8:451–458. [PubMed: 19839936]

Hu LA, Tang Y, Miller WE, Cong M, Lau AG, Lefkowitz RJ, Hall RA. beta 1-adrenergic receptor association with PSD-95. Inhibition of receptor internalization and facilitation of beta 1-adrenergic receptor interaction with N-methyl-D-aspartate receptors. J. Biol. Chem. 2000; 275:38659–38666. [PubMed: 10995758]

Hudson BD, Hebert TE, Kelly ME. Physical and functional interaction between CB1 cannabinoid receptors and beta2-adrenoceptors. Br. J. Pharmacol. 2010; 160:627–642. [PubMed: 20590567]

Jensen BC, Swigart PM, Simpson PC. Ten commercial antibodies for alpha-1-adrenergic receptor subtypes are nonspecific. Naunyn Schmiedebergs Arch. Pharmacol. 2009; 379:409–412. [PubMed: 18989658]

Jewell-Motz EA, Donnelly ET, Eason MG, Liggett SB. Agonist-mediated downregulation of G alpha i via the alpha 2-adrenergic receptor is targeted by receptor-Gi interaction and is independent of receptor signaling and regulation. Biochemistry. 1998; 37:15720–15725. [PubMed: 9843377]

Jones SB, Leone SL, Bylund DB. Desensitization of the alpha-2 adrenergic receptor in HT29 and opossum kidney cell lines. J. Pharmacol. Exp. Ther. 1990; 254:294–300. [PubMed: 2164096]

Katona I, Urban GM, Wallace M, Ledent C, Jung KM, Piomelli D, Mackie K, Freund TF. Molecular composition of the endocannabinoid system at glutamatergic synapses. J. Neurosci. 2006; 26:5628–5637. [PubMed: 16723519]

Kirby LG, Freeman-Daniels E, Lemos JC, Nunan JD, Lamy C, Akanwa A, Beck SG. Corticotropin-releasing factor increases GABA synaptic activity and induces inward current in 5-hydroxytryptamine dorsal raphe neurons. J. Neurosci. 2008; 28:12927–12937. [PubMed: 19036986]

Kuzmiski JB, Pittman QJ, Bains JS. Metaplasticity of hypothalamic synapses following in vivo challenge. Neuron. 2009; 62:839–849. [PubMed: 19555652]

Lapiz MD, Morilak DA. Noradrenergic modulation of cognitive function in rat medial prefrontal cortex as measured by attentional set shifting capability. Neuroscience. 2006; 137:1039–1049. [PubMed: 16298081]

Leranth, C.; Pickel, VM. Electron microscopic preembedding double-labeling methods. In: Heimer, L.; Zaborszky, L., editors. Neuroanatomical tracing methods 2. New York: Plenum Press; 1989. p. 129-172.

Li BM, Mao ZM, Wang M, Mei ZT. Alpha-2 adrenergic modulation of prefrontal cortical neuronal activity related to spatial working memory in monkeys. Neuropsychopharmacology. 1999; 21:601–610. [PubMed: 10516956]

Liggett SB, Ostrowski J, Chesnut LC, Kurose H, Raymond JR, Caron MG, Lefkowitz RJ. Sites in the third intracellular loop of the alpha 2A–adrenergic receptor confer short term agonist-promoted desensitization. Evidence for a receptor kinase-mediated mechanism. J. Biol. Chem. 1992; 267:4740–4746. [PubMed: 1311318]

Lu R, Li Y, Zhang Y, Chen Y, Shields AD, Winder DG, Angelotti T, Jiao K, Limbird LE, Zhou Y, Wang Q. Epitope-tagged receptor knock-in mice reveal that differential desensitization of alpha2-adrenergic responses is because of ligand-selective internalization. J. Biol. Chem. 2009; 284:13233–13243. [PubMed: 19276088]

Matthews GA, Patel R, Walsh A, Davies O, Martinez-Ricos J, Brennan PA. Mating increases neuronal tyrosine hydroxylase expression and selectively gates transmission of male chemosensory information in female mice. PLoS One. 2013; 8:e69943. [PubMed: 23936125]

McCune SK, Voigt MM, Hill JM. Expression of multiple alpha adrenergic receptor subtype messenger RNAs in the adult rat brain. Neuroscience. 1993; 57:143–151. [PubMed: 8278048]

Meana JJ, Barturen F, Garcia-Sevilla JA. Alpha 2-adrenoceptors in the brain of suicide victims: increased receptor density associated with major depression. Biol. Psychiatry. 1992; 31:471–490. [PubMed: 1349830]

Miller EK, Cohen JD. An integrative theory of prefrontal cortex function. Annu. Rev. Neurosci. 2001; 24:167–202. [PubMed: 11283309]

Milligan G, Wise A, MacEwan DJ, Grassie MA, Kennedy FR, Lee TW, Adie EJ, Kim GD, McCallum JF, Burt A&. Mechanisms of agonist-induced G-protein elimination. Biochem. Soc. Trans. 1995; 23:166–170. [PubMed: 7758721]

Nicholas AP, Pieribone V, Hokfelt T. Distributions of mRNAs for alpha-2 adrenergic receptor subtypes in rat brain: an in situ hybridization study. J. Comp Neurol. 1993; 328:575–594. [PubMed: 8381444]

Oropeza VC, Mackie K, Van Bockstaele EJ. Cannabinoid receptors are localized to noradrenergic axon terminals in the rat frontal cortex. Brain Res. 2007; 1127:36–44. [PubMed: 17113043]

Oropeza VC, Page ME, Van Bockstaele EJ. Systemic administration of WIN 55,212-2 increases norepinephrine release in the rat frontal cortex. Brain Res. 2005; 1046:45–54. [PubMed: 15927549]

Page ME, Oropeza VC, Sparks SE, Qian Y, Menko AS, Van Bockstaele EJ. Repeated cannabinoid administration increases indices of noradrenergic activity in rats. Pharmacol. Biochem. Behav. 2007; 86:162–168. [PubMed: 17275893]

Page ME, Oropeza VC, Van Bockstaele EJ. Local administration of a cannabinoid agonist alters norepinephrine efflux in the rat frontal cortex. Neurosci Lett. 2008; 431:1–5. [PubMed: 18055114]

Pattij T, Wiskerke J, Schoffelmeer AN. Cannabinoid modulation of executive functions. Eur. J. Pharmacol. 2008; 585:458–463. [PubMed: 18423599]

Peters A, Palay SL. The morphology of synapses. J. Neurocytol. 1996; 25:687–700. [PubMed: 9023718]

Peters, A.; Palay, SL.; Webster, HD. The fine structure of the nervous system. New York: Oxford University Press; 1991.

Polanski W, Enzensperger C, Reichmann H, Gille G. The exceptional properties of 9-methyl-beta-carboline: stimulation, protection and regeneration of dopaminergic neurons coupled with anti-inflammatory effects. J. Neurochem. 2010; 113:1659–1675. [PubMed: 20374418]

Pradidarcheep W, Stallen J, Labruyere WT, Dabhoiwala NF, Michel MC, Lamers WH. Lack of specificity of commercially available antisera against muscarinergic and adrenergic receptors. Naunyn Schmiedebergs Arch. Pharmacol. 2009; 379:397–402. [PubMed: 19198807]

Pudovkina OL, Kawahara Y, de VJ, Westerink BH. The release of noradrenaline in the locus coeruleus and prefrontal cortex studied with dual-probe microdialysis. Brain Res. 2001; 906:38–45. [PubMed: 11430860]

Ramos BP, Arnsten AF. Adrenergic pharmacology and cognition: focus on the prefrontal cortex. Pharmacol. Ther. 2007; 113:523–536. [PubMed: 17303246]

Ranganathan M, D'Souza DC. The acute effects of cannabinoids on memory in humans: a review. Psychopharmacology (Berl). 2006; 188:425–444. [PubMed: 17019571]

Reyes BA, Rosario JC, Piana PM, Van Bockstaele EJ. Cannabinoid modulation of cortical adrenergic receptors and transporters. J. Neurosci Res. 2009; 87:3671–3678. [PubMed: 19533736]

Reyes BA, Szot P, Sikkema C, Cathel AM, Kirby LG, Van Bockstaele EJ. Stress-induced sensitization of cortical adrenergic receptors following a history of cannabinoid exposure. Exp. Neurol. 2012; 236:327–335. [PubMed: 22677142]

Richter H, Teixeira FM, Ferreira SG, Kittel A, Kofalvi A, Sperlagh B. Presynaptic alpha(2)-adrenoceptors control the inhibitory action of presynaptic CB(1) cannabinoid receptors on prefrontocortical norepinephrine release in the rat. Neuropharmacology. 2012; 63:784–797. [PubMed: 22722024]

Robbins TW. Cortical noradrenaline, attention and arousal. Psychol. Med. 1984; 14:13–21. [PubMed: 6709778]

Scavone JL, Mackie K, Van Bockstaele EJ. Characterization of cannabinoid-1 receptors in the locus coeruleus: relationship with mu-opioid receptors. Brain Res. 2010; 1312:18–31. [PubMed: 19931229]

Scheinin M, Lomasney JW, Hayden-Hixson DM, Schambra UB, Caron MG, Lefkowitz RJ, Fremeau RT Jr. Distribution of alpha 2-adrenergic receptor subtype gene expression in rat brain. Mol. Brain Res. 1994; 21:133–149. [PubMed: 8164514]

Strader CD, Pickel VM, Joh TH, Strohsacker MW, Shorr RG, Lefkowitz RJ, Caron MG. Antibodies to the beta-adrenergic receptor: attenuation of catecholamine-sensitive adenylate cyclase and demonstration of postsynaptic receptor localization in brain. Proc. Natl Acad. Sci USA. 1983; 80:1840–1844. [PubMed: 6300875]

Verrico CD, Jentsch JD, Roth RH. Persistent and anatomically selective reduction in prefrontal cortical dopamine metabolism after repeated, intermittent cannabinoid administration to rats. Synapse. 2003; 49:61–66. [PubMed: 12710016]

Wang M, Ramos BP, Paspalas CD, Shu Y, Simen A, Duque A, Vijayraghavan S, Brennan A, Dudley A, Nou E, Mazer JA, McCormick DA, Arnsten AF. Alpha2A–adrenoceptors strengthen working memory networks by inhibiting cAMP-HCN channel signaling in prefrontal cortex. Cell. 2007; 129:397–410. [PubMed: 17448997]

Wang RX, Limbird LE. Distribution of mRNA encoding three alpha 2-adrenergic receptor subtypes in the developing mouse embryo suggests a role for the alpha 2A subtype in apoptosis. Mol. Pharmacol. 1997; 52:1071–1080. [PubMed: 9415717]

Westerink BH, Kawahara Y, De BP, Geels C, De Vries JB, Wikstrom HV, Van KA, Van VB, Kruse CG, Long SK. Antipsychotic drugs classified by their effects on the release of dopamine and noradrenaline in the prefrontal cortex and striatum. Eur. J. Pharmacol. 2001; 412:127–138. [PubMed: 11165224]

Winzer-Serhan UH, Leslie FM. Expression of alpha2A adrenoceptors during rat neocortical development. J. Neurobiol. 1999; 38:259–269. [PubMed: 10022571]

Witkin JM, Tzavara ET, Nomikos GG. A role for cannabinoid CB1 receptors in mood and anxiety disorders. Behav. Pharmacol. 2005; 16:315–331. [PubMed: 16148437]

Zhang W, Perry KW, Wong DT, Potts BD, Bao J, Tollefson GD, Bymaster FP. Synergistic effects of olanzapine and other antipsychotic agents in combination with fluoxetine on norepinephrine and dopamine release in rat prefrontal cortex. Neuropsychopharmacology. 2000; 23:250–262. [PubMed: 10942849]

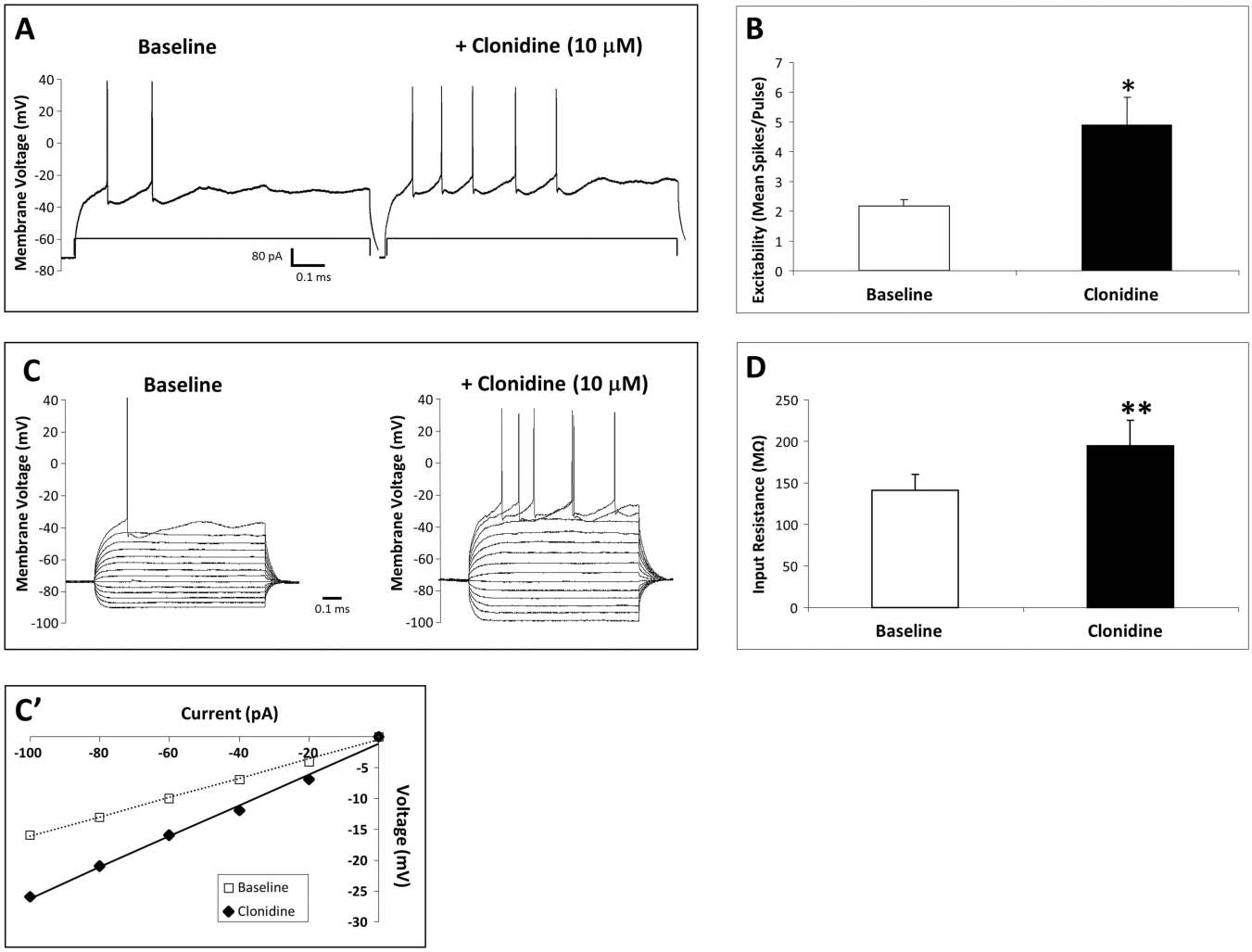

Fig. 1.

α2-AR-mediated increase in mPFC pyramidal neuron excitability and input resistance. *In-vitro* clonidine (10 μM) elevated excitability in an individual neuron from 2 to 5 spikes/pulse (A) and significantly elevated mean excitability (B) (N = 6 cells). Clonidine also elevated membrane input resistance in an individual neuron from 157 to 251 MΩ, as shown by voltage responses to a series of hyperpolarizing to depolarizing current steps (C) and in a current–voltage plot (C′), and significantly elevated mean input resistance (D) (N = 6 cells). Significant change from baseline by paired Student's t-test (*$p < 0.05$, **$p < 0.01$). Data are represented as mean + SEM.

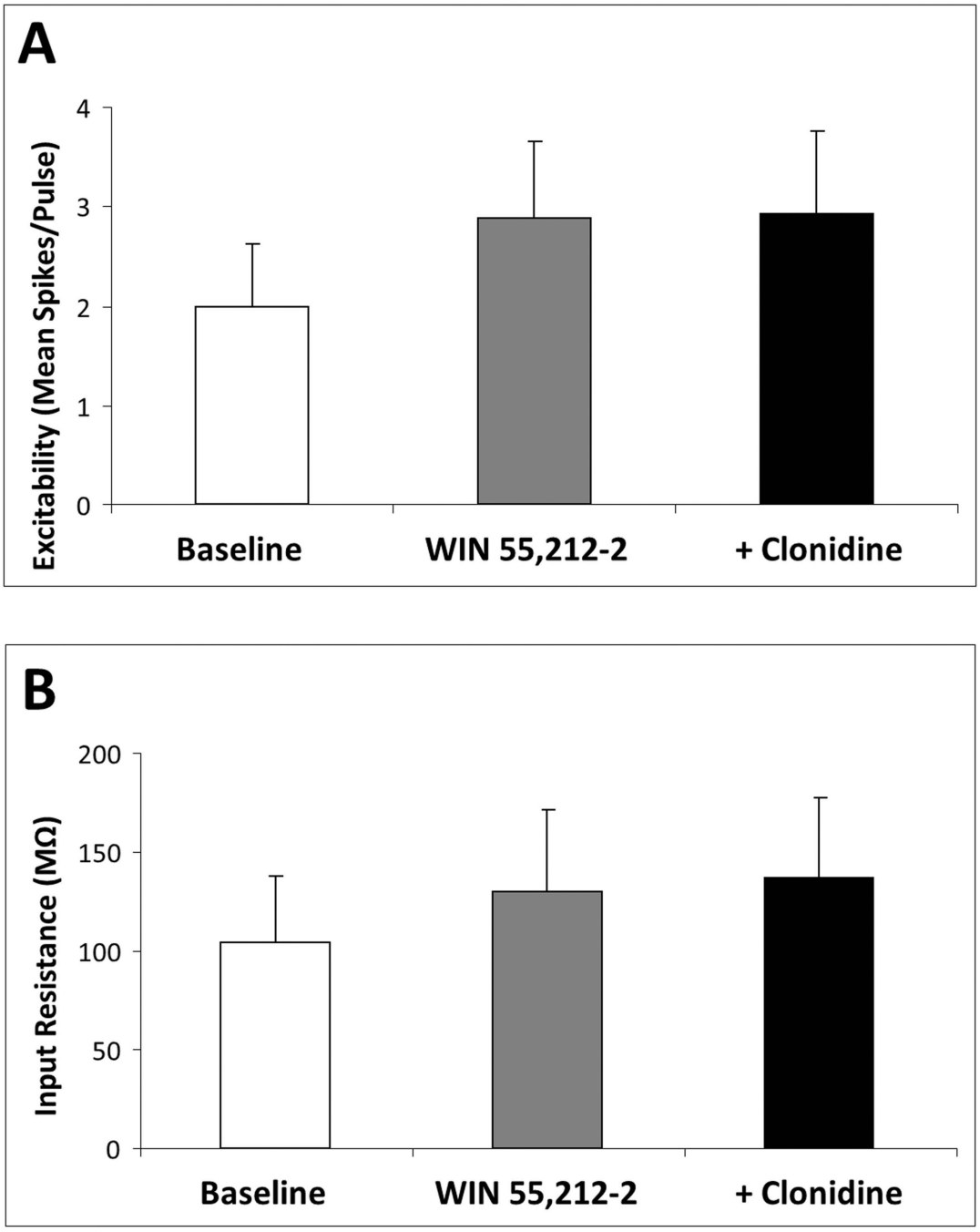

Fig. 2.

Acute CB1R stimulation blocks α2-AR-mediated increase in mPFC pyramidal neuron excitability and input resistance. Acute *in-vitro* pretreatment with the CB1 agonist WIN 55,212-2 (1.0 μM) blocks clonidine (10 μM)-induced elevation of mPFC pyramidal neuron excitability (N = 7 cells) (A) and input resistance (N = 9 cells) (B). Data are represented as mean + SEM.

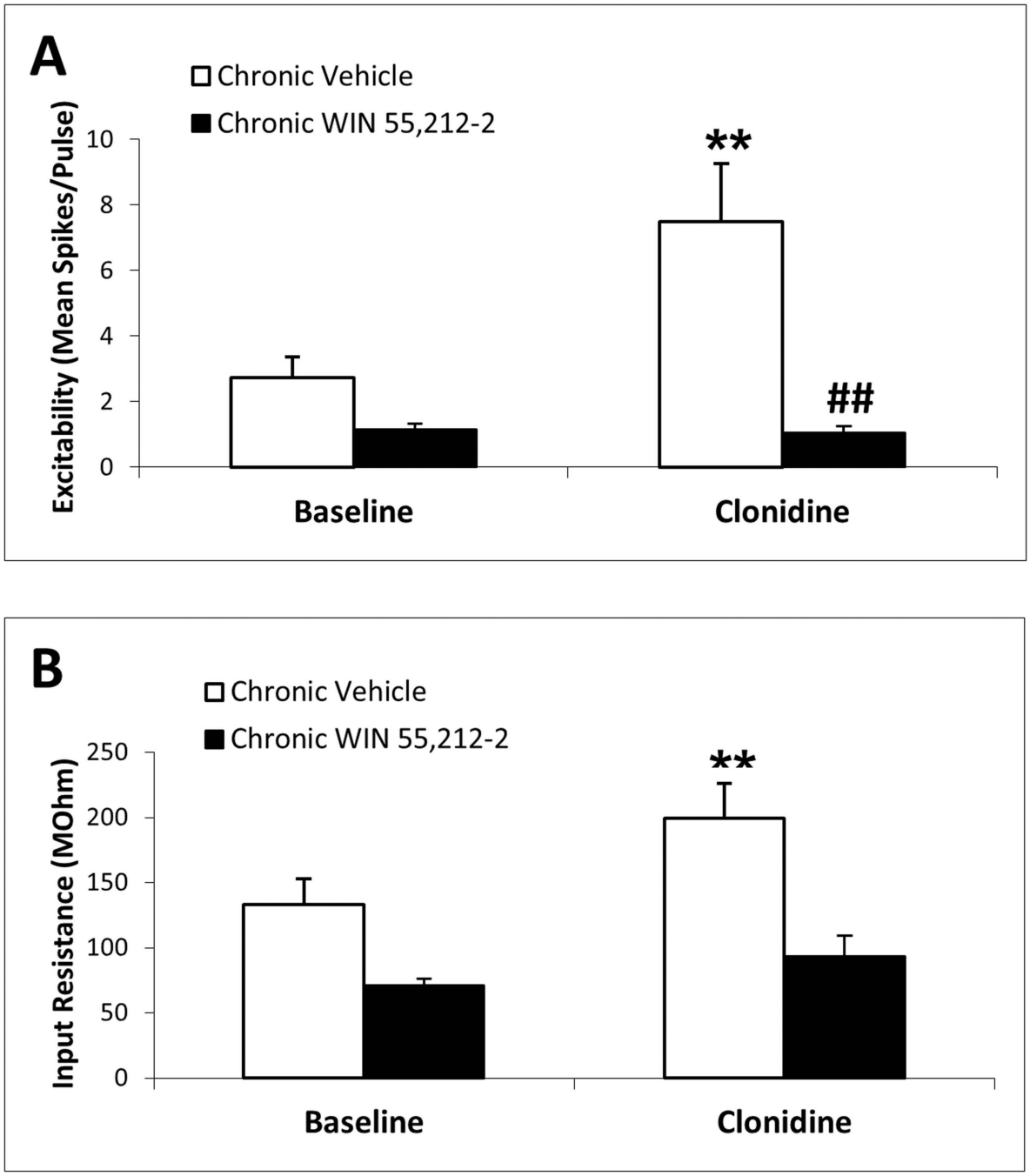

Fig. 3.

Chronic CB1R stimulation blocks α2-AR-mediated increase in mPFC pyramidal neuron excitability and input resistance. Chronic *in-vivo* pretreatment with the CB1 agonist WIN 55,212-2 (3 mg/kg, i.p., once daily for 7 days) blocks *in-vitro* clonidine (10 mM)-induced elevation of mPFC pyramidal neuron excitability and input resistance. In slices from subjects treated with chronic vehicle, clonidine increases mean mPFC neuron excitability (N = 17 cells) (A) and input resistance (N = 17 cells) (B). In slices from subjects treated with chronic WIN 55,212-2, clonidine has no effect on mPFC neuron excitability (N = 10 cells)

(A) or input resistance (N = 9 cells) (B). Significant change from baseline by posthoc Student–Newman–Keuls test (**$p < 0.01$) and significant difference from chronic vehicle controls by posthoc Student–Newman–Keuls test (##$p < 0.01$). Data are represented as mean + SEM.

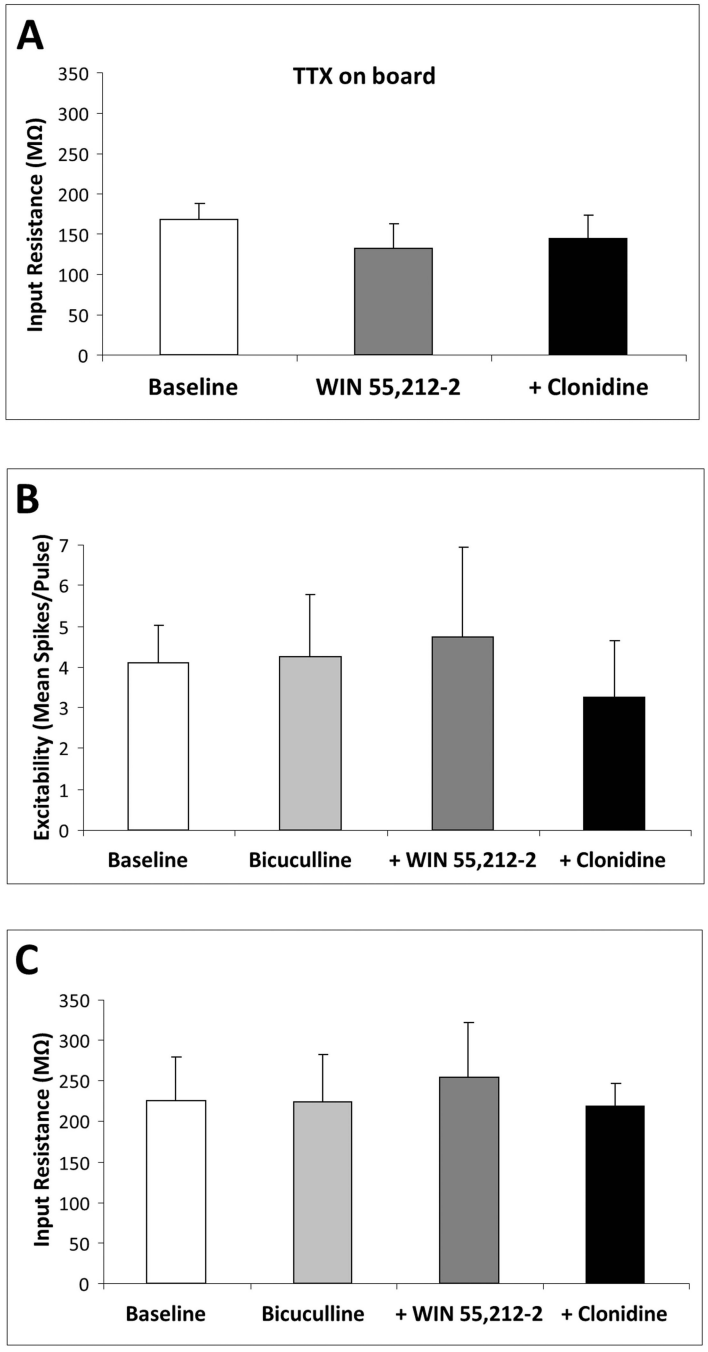

Fig. 4.

CB1–α2-AR interactions in mPFC pyramidal neurons are action potential- and GABA-independent. In the presence of the Na^+ channel inhibitor TTX (1 μM), acute *in-vitro* WIN 55,212-2 (1 μM) blocks *in-vitro* clonidine (10 μM)-induced elevation of mPFC pyramidal neuron input resistance (N = 9 cells) (A). Pretreatment with the $GABA_A$ receptor antagonist bicuculline (20 μM) does not prevent acute WIN 55,212-2 (1 μM) from blocking clonidine (10 μM)-induced elevation of mPFC pyramidal neuron excitability (N = 7 cells) (B) and input resistance (N = 7 cells) (C). Data are represented as mean + SEM.

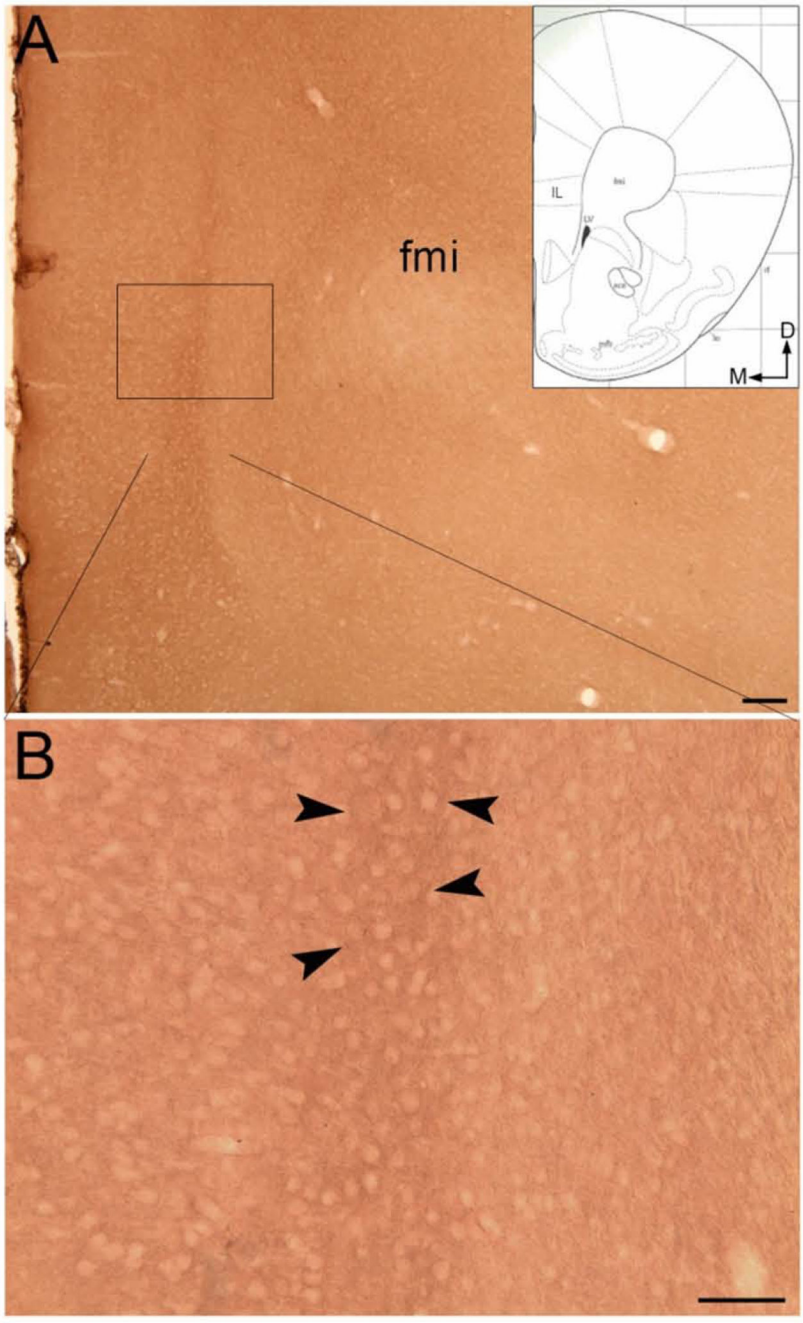

Fig. 5.

(A and B) Brightfield photomicrographs showing immunoperoxidase labeling of HA-α2A-AR immunoreactivity in the mPFC. Dense peroxidase labeling can be seen in the region of the infralimbic cortex (arrowheads). Arrows indicate dorsal (D) and medial (M) orientation of the tissue section. Inset: a schematic illustration adapted from the mouse brain stereotaxic coordinates (Franklin & Paxinos, 2008) showing the anterior–posterior level from which the photomicrographs in A and B are taken. The region denoted by the box in A can be seen at higher magnification in B. aca, anterior commissure, anterior; fmi, forceps minor corpus

callosum; IL, infralimbic cortex; lo, lateral olfactory tract; LV, lateral ventricle; mfb, medial forebrain bundle; rf, rhinal fissure. Scale bars: A, 100 μm; B, 50 μm.

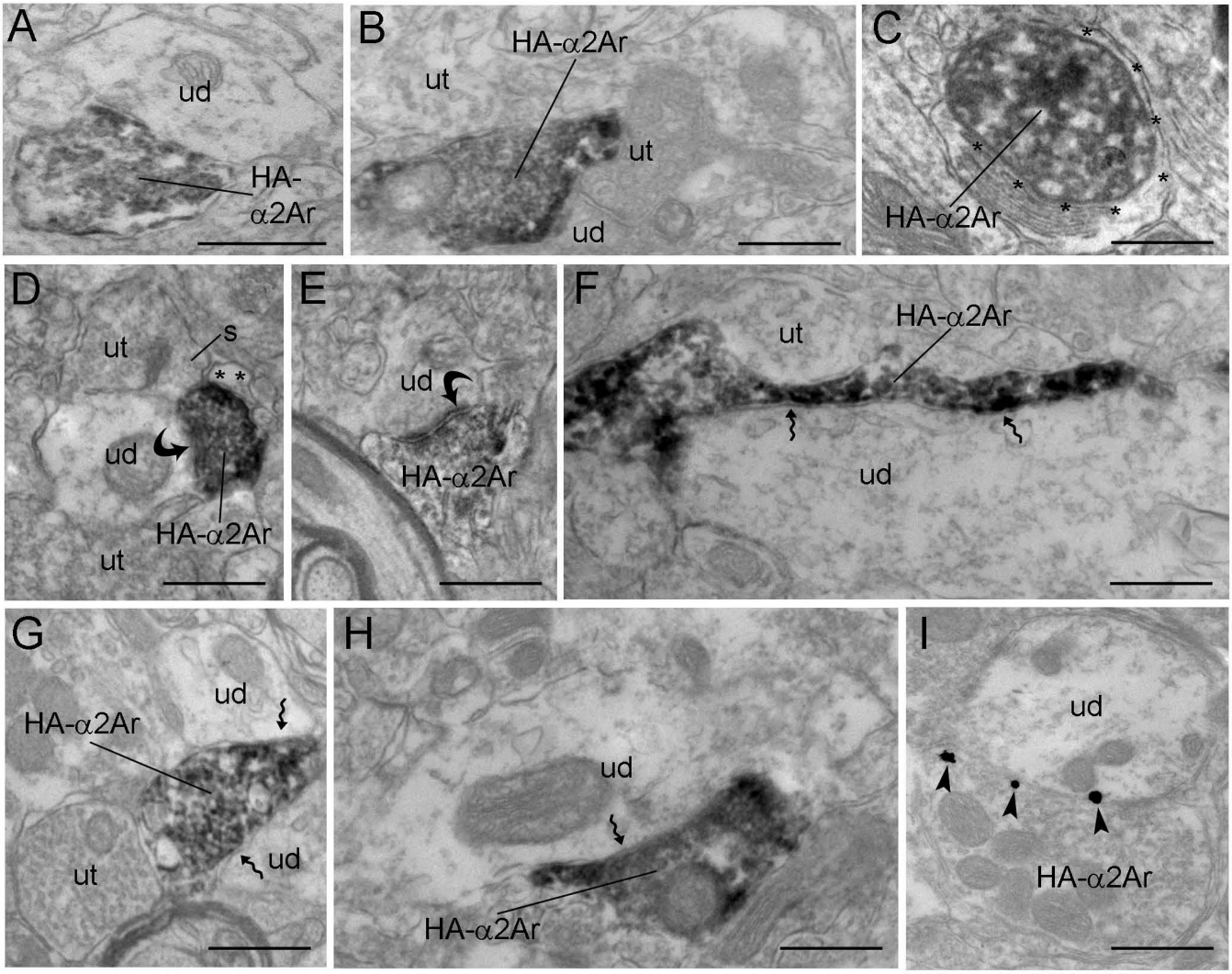

Fig. 6.

Electron micrographs showing immunoperoxidase and immunogold–silver labeling for HA-α2A-AR in axon terminals in the mPFC. (A and D–H) Peroxidase labeling for HA-α2A-AR in axon terminals (HA-α2Art) that are in direct contact with unlabeled dendrites (ud) in the mPFC. In these synaptic contact arrangements, some HA-α2Art form visible asymmetric (curved arrow, D and E) or symmetric (zigzag arrow, F–H) synapses, whereas other appositions are difficult to unequivocally establish in the plane of section analyzed and are classified as ‘undefined’ (A and B). Some HA-α2Art are directly apposed to unlabeled axon terminals (ut) (B, F and G) or converge on common dendrites with unlabeled axon terminals (B and D). Peroxidase-labeled HA-α2A-AR axon terminals are also apposed by astrocytic processes (*) (C and D). (I) Electron micrograph showing immunogold–silver labeling (arrowheads) for HA-α2A-AR in an axon terminal that is in direct contact with an unlabeled dendrite (ud). The unlabeled dendrite receives convergent input from a ut. Scale bars, 0.5 μm.

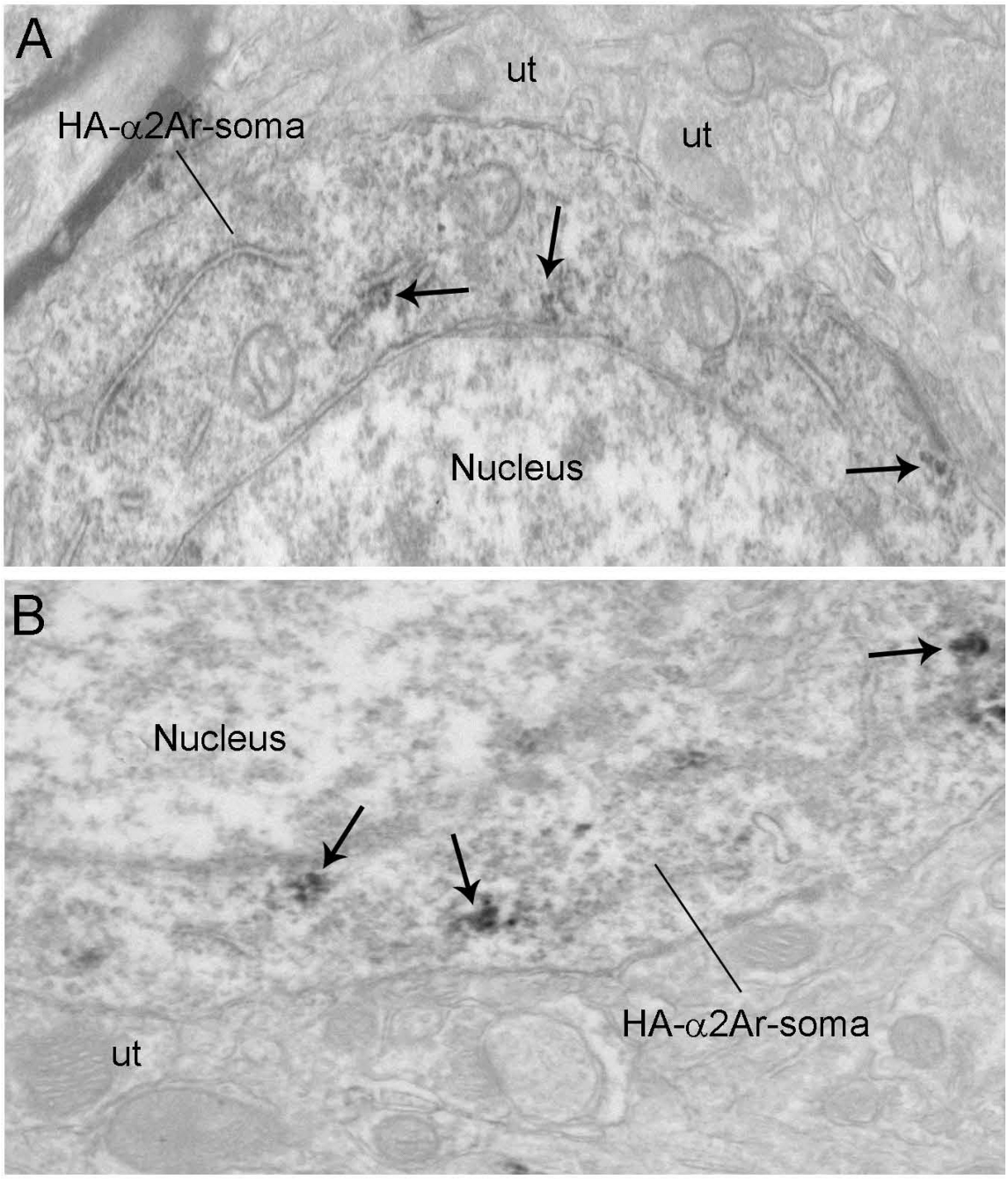

Fig. 7.

(A and B) Electron micrographs showing immunoperoxidase labeling for HA-α2A-AR in somata in the mPFC. HA-α2A-AR immunoreactivity appeared as discrete clumps near the rough endoplasmic reticulum and along the intracellular surface of the plasma membrane (black arrows) in the somata. The intracellular surfaces of somatic plasma membranes were also labeled. These patches of immunoreactive plasma membranes were sometimes associated with synapses. Scale bars, 0.5 μm.

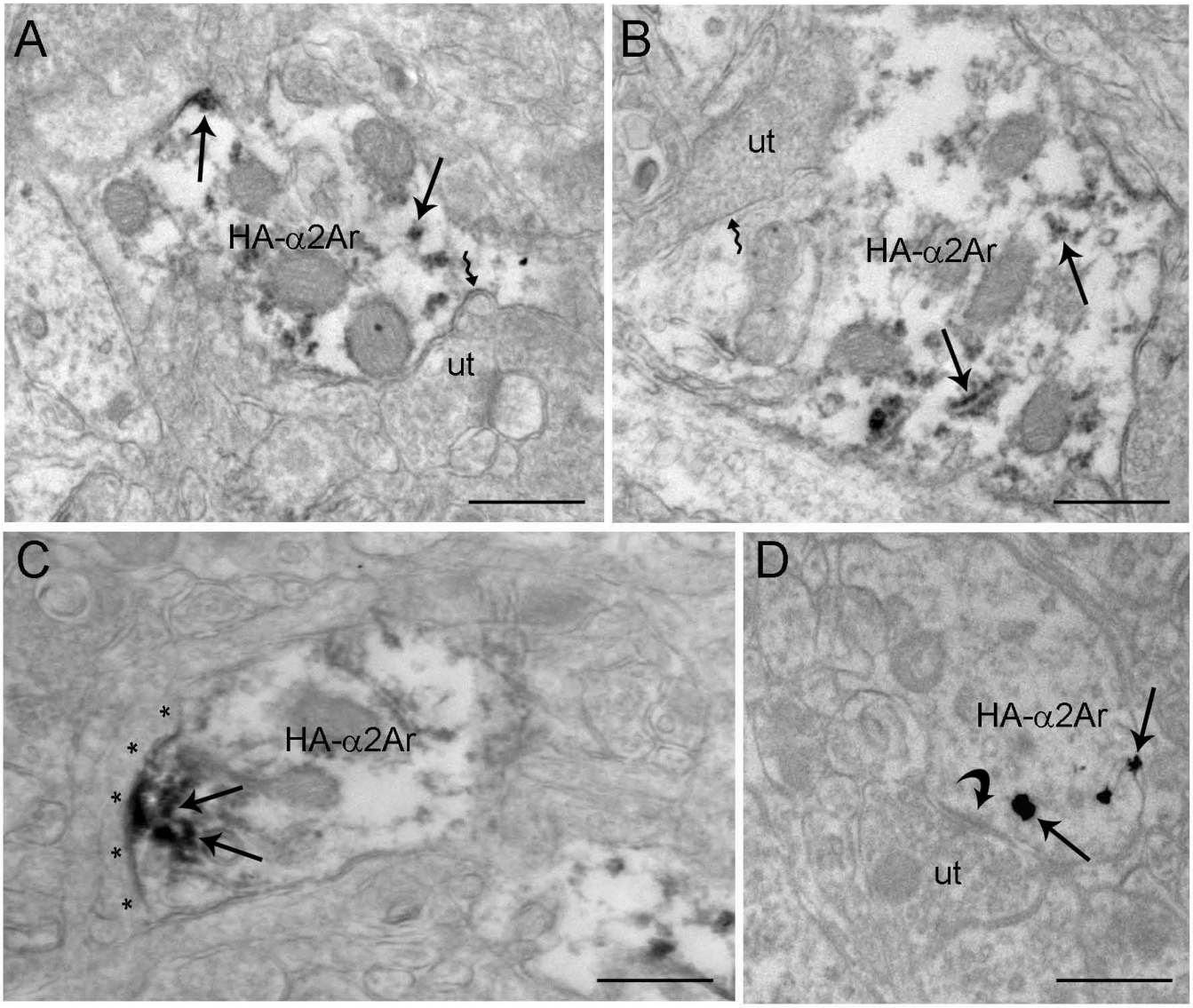

Fig. 8.

Electron micrographs showing immunoperoxidase labeling for HA-α2A-AR in dendritic processes in the mPFC. Unlabeled axon terminals (ut) formed either asymmetric (curved arrow, B) or symmetric (A and D) synapses with HA-α2A-AR-labeled dendrites. Arrows depict HA-α2A-AR immunoreactivity in dendrites. (B) HA-α2A-AR-labeled dendrite (HA-d) receiving an asymmetric synapse (curved arrow) from an unlabeled axon terminal (ut). Arrows depict HA-α2A-AR immunogold–silver particles. Scale bars, 0.5 μm.

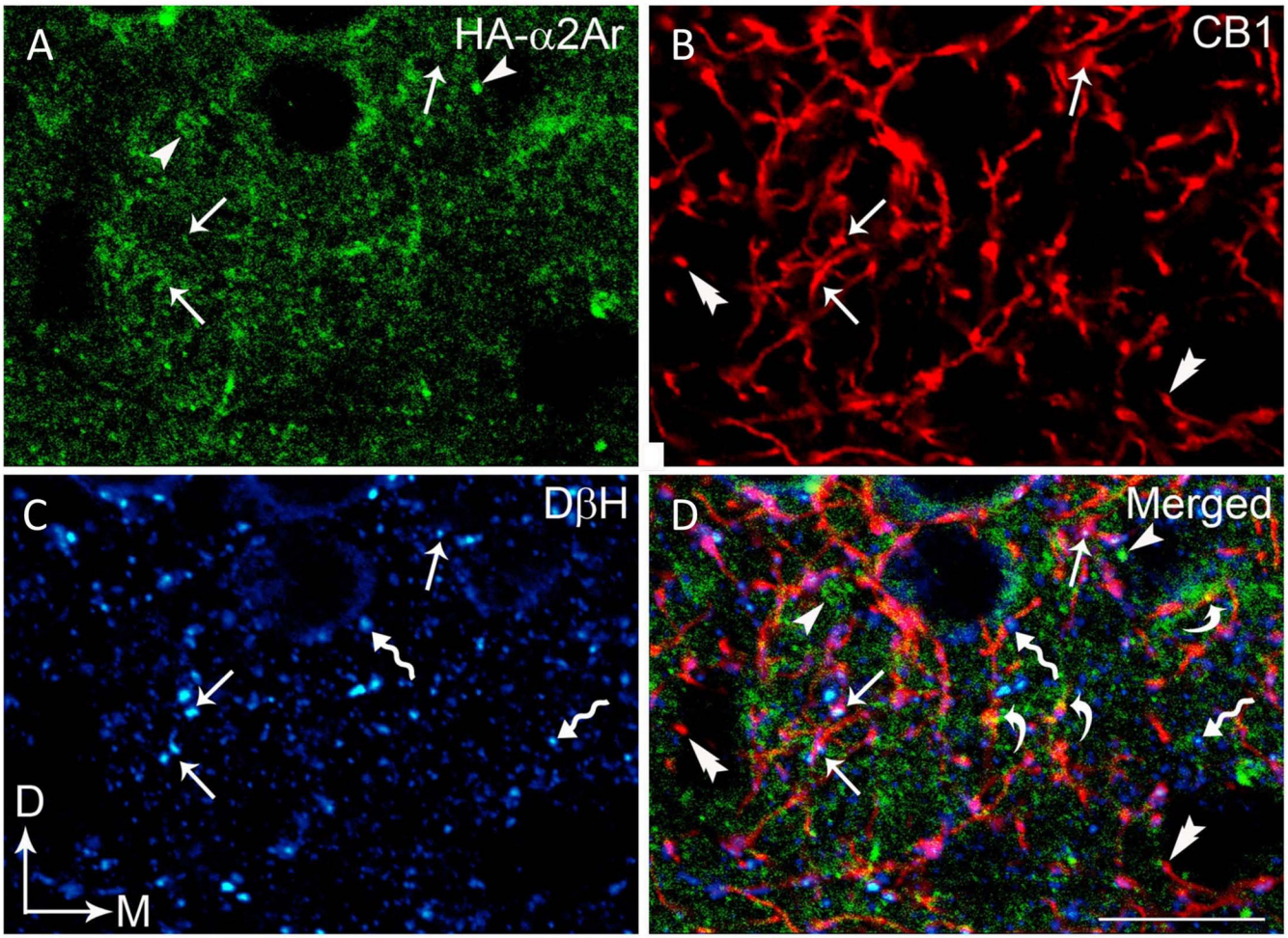

Fig. 9.

Confocal immunofluorescence photomicrographs showing triple labeling for HA-α2-AR, CB1R, and DβH in a coronal section through the mPFC. HA-α2-AR immunoreactivity was labeled with fluorescein isothiocyanate (green), CB1R was labeled with rhodamine isothiocyanate (red) and DβH was labeled with Cy5 (blue). Arrows depict triple labeling for HA-α2-AR (A), CB1R (B) and DβH (C), whereas arrowheads, double arrowheads, and zigzag arrows depict singly-labeled HA-α2-AR, CB1R and DβH, respectively. (D) Merged image. Scale bar, 25 μm.